Rubrene Cation Radical Stabilized by Polyiodide Chains in the (Rubrene)I_9 Crystal

Megumi Kameya, Toshio Naito, and Tamotsu Inabe*

Division of Chemistry, Graduate School of Science, Hokkaido University, Sapporo 060-0810

(Received August 26, 1999)

A fused polycyclic aromatic compound, rubrene (RB), has been found to form a charge-transfer compound with iodine with the stoichiometry of RB·I_9. The crystal is monoclinic, space group $C2/c$, a = 14.482(4), b = 16.676(8), c = 19.985(4) Å, β = 106.90(2)°, V = 4618(2) Å^3, and Z = 4. In this crystal, a unique branched crank-shaped one-dimensional $(I_9^-)_\infty$ polyiodide chain is formed. RB is surrounded by the polyiodide, and its cation radical state, which is unstable under normal conditions, is stabilized. The formation of the RB cation radical has been confirmed by IR, VIS-NIR, and EPR spectroscopies. The magnetic susceptibility measurement has indicated the existence of superexchange interactions through the polyiodide.

Many aromatic hydrocarbons are known to form charge-transfer complexes with various acceptors. Depending on the acceptor strength (electron affinity) and the donor strength (ionization potential, IP), the ground state of the complex varies from neutral to ionic one. In general, the ionization potential of linearly annulated polyacenes decreases with increasing the number of the condensed rings.[1] For example, the IP values of benzene, naphthalene, anthracene, and naphthacene have been reported to be 9.24, 8.15, 7.40, and 7.01 eV, respectively. The value of naphthacene is still higher than those of typical donor molecules for molecular conductors such as TTT (tetrathianaphthacene, 6.2 eV),[2] TTF (tetrathiafulvalene, 6.92 eV),[3,4] TMTTF (tetramethyltetrathiafulvalene, 6.38 eV),[3] etc. Interestingly, the introduction of phenyl groups to naphthacene results in a substantial decrease of its IP value; the IP value of 5,6,11,12-tetraphenylnaphthacene, RB (Chart 1), is only 6.52 eV.[1] This value makes one expect that RB can be a good donor component. However, so far, no charge-transfer complexes based on the RB donor have been reported. This may be due to its largely non-planar shape which makes it impossible for the π-electrons to overlap with the π-acceptors. The non-planarity may be disadvantageous for the simple π–π stacking interaction. However, if one molecule has several π-conjugated planes oriented in different directions, the π–π interactions in the whole crystal may become different from those observed in simple one-dimensional conductors. Thus, we have approached the construction of the RB molecular complex by combining with various anions, since the cation radical species was detected in the solution.[5] Though the molecule can easily be oxidized chemically or electrochemically, the radical species is short-lived in the solution. The first RB cation radical crystal has been found to be obtained when the crystal growth is carried out by slow evaporation of the solution containing RB and an excess amount of iodine. In this paper, we describe the crystal structure thus obtained and the unique polyiodide form found in this crystal.

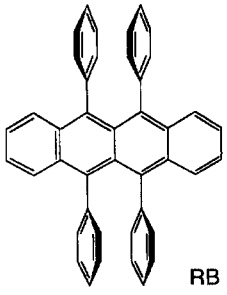

Chart 1.

Experimental

Materials. The RB·I_9 single crystals were obtained as follows. A saturated benzene solution containing 31.8 mg (0.0597 mmol) of RB and 73.6 mg (0.290 mmol) of I_2 in a beaker with a loose cover was kept standing for several days. Black needles were obtained on the bottom surface of the beaker. The crystals lose iodine gradually in the open air, and were stored in a sealed container with pieces of iodine at 4 °C.

X-Ray Structure Analysis. Since the crystal is not so stable in the air, the measurements were performed with a crystal sealed in a capillary tube with a small piece of iodine. An automated Rigaku AFC-7R diffractometer with graphite-monochromated Mo $K\alpha$ radiation was used for data collection at 293 K. The data-collection conditions are summarized in Table 1. Three standard reflections, which were monitored every 150 data measurements, showed a gradual decrease in intensities (to end up with 71.8% of the initial intensity; the decay correction was applied). This situation set a limit to the 2θ range of the data collection. The absorption correction was applied by a ψ-scan method. The structure was solved by a direct method (SIR-92[6]), and the hydrogen atoms were placed at the calculated ideal positions. A full-matrix least-squares technique

Table 1. Data-Collection Conditions and Crystal Data of RB·I_9

Chemical formula	$C_{42}H_{28}I_9$
Molecular weight	1674.82
Crystal size/mm	$0.30 \times 0.13 \times 0.05$
Crystal system	Monoclinic
Space group	$C2/c$
a/Å	14.482(4)
b/Å	16.676(8)
c/Å	19.985(4)
β/°	106.90(2)
V/Å^3	4618(2)
Z	4
D_{calc}/g cm^{-3}	2.409
μ(Mo $K\alpha$)/cm^{-1}	60.72
2θ range/°	$5 < 2\theta < 48$
Scan width/degrees	$1.78+0.30 \tan\theta$
Scan mode	ω–2θ
Scan rate/degrees min^{-1}	16
No. of reflections measured	3749
No. of independent reflections observed	1417 [$I > 3\sigma(I)$]
No. of parameters	232
R	0.054
R_w	0.053

with anisotropic thermal parameters for non-hydrogen atoms and isotropic ones for hydrogen atoms (thermal parameters are 1.2 times of the attached carbons) was employed for the structure refinement (TEXSAN[7]).

Crystallographic data have been deposited at the CCDC, 12 Union Road, Cambridge CB2 1EZ, UK and copies can be obtained on request, free of charge, by quoting the publication citation and the deposition numbers CCDC 135923.

Measurements. The infrared spectra of the KBr pellet samples were measured using a Perkin–Elmer 1650 FT-IR spectrometer. The visible-near-IR spectra were recorded on a JASCO V-570 spectrometer. For the solid samples, the diffuse reflectance diluted with KBr was measured. The spectra were then plotted using the Kubelka-Munk function. The X-band EPR spectrum of the randomly oriented polycrystalline sample was measured using a JEOL FE1X spectrometer. The magnetic susceptibility was measured by a Quantum Design MPMS-5S SQUID susceptometer.

Results and Discussion

Molecular and Crystal Structure of RB·I_9. Figure 1 shows the RB molecular structure in RB·I_9. Atomic parameters are listed in Table 2.[8] A two-fold axis perpendicular to the naphthacene ring passes through the center of the molecule. Though the RB molecule in the single component crystal also has the same symmetry element, it operates differently; the two-fold axis coincides with the central C–C bond.[9] In the single component crystal, the naphthacene ring is nearly planar. On the other hand, the naphthacene ring of RB in RB·I_9 is twisted by 27.0°. Two pairs of the face-to-face phenyl groups alternately stick out of the naphthacene plane. This is due to the steric interaction between the phenyl rings, and the C(10)···C(16) nonbonded distance is still very short (2.88(3) Å). Similarly, the face-to-face pairs of the phenyl groups in the single component crystal stick out of the naphthacene plane,[9] as shown in Fig. 2. However, the relative

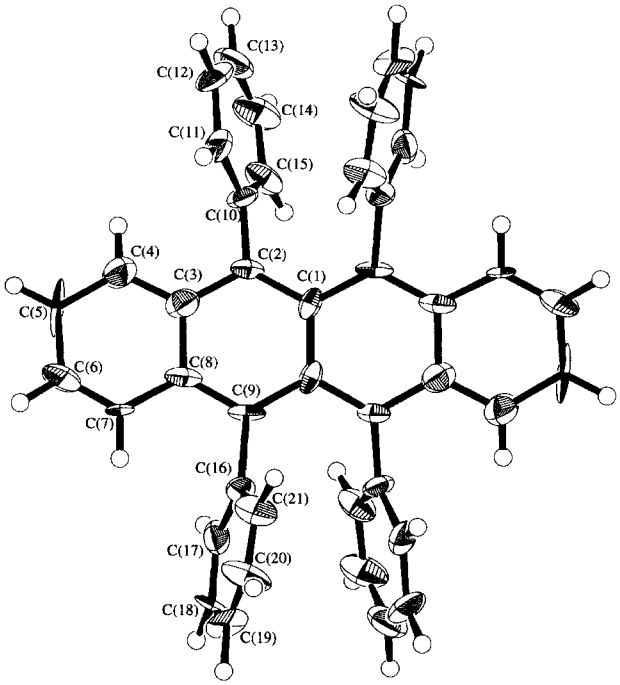

Fig. 1. ORTEP drawing of RB in RB·I_9 showing the atom numbering scheme.

Table 2. Fractional Coordinates and Equivalent Temperature Factors for RB·I_9

Atom	x	y	z	B_{eq}/Å^2
I(1)	1.0000	0.5000	1.0000	5.90(8)
I(2)	0.9923(2)	0.3253(1)	0.9896(1)	7.11(7)
I(3)	1.0727(2)	−0.1104(1)	0.8541(1)	8.47(8)
I(4)	1.2613(1)	−0.1422(1)	0.9172(1)	6.70(6)
I(5)	0.9987(1)	0.3388(1)	0.8182(1)	5.59(5)
C(1)	0.952(1)	0.112(1)	0.755(1)	2.2(5)
C(2)	0.943(1)	0.102(1)	0.822(1)	2.2(6)
C(3)	1.025(2)	0.108(1)	0.883(1)	3.3(7)
C(4)	1.019(2)	0.099(2)	0.950(1)	4.1(7)
C(5)	1.100(2)	0.114(2)	1.008(1)	6.0(9)
C(6)	1.189(2)	0.134(2)	0.995(2)	6.1(9)
C(7)	1.197(1)	0.138(2)	0.933(1)	4.3(7)
C(8)	1.119(1)	0.124(1)	0.873(1)	3.0(6)
C(9)	1.128(1)	0.122(1)	0.805(1)	2.1(6)
C(10)	0.853(1)	0.077(1)	0.836(1)	2.6(6)
C(11)	0.800(2)	0.124(2)	0.867(1)	3.9(7)
C(12)	0.713(2)	0.097(2)	0.879(1)	5.6(9)
C(13)	0.684(2)	0.019(2)	0.862(1)	4.8(8)
C(14)	0.736(2)	−0.030(2)	0.832(1)	4.9(8)
C(15)	0.816(2)	0.000(2)	0.817(1)	3.8(7)
C(16)	1.229(1)	0.142(1)	0.802(1)	2.6(6)
C(17)	1.305(2)	0.088(2)	0.820(1)	3.5(6)
C(18)	1.394(2)	0.115(2)	0.817(1)	5.6(9)
C(19)	1.409(2)	0.192(2)	0.799(1)	5(1)
C(20)	1.338(2)	0.244(2)	0.785(2)	5.6(9)
C(21)	1.248(2)	0.219(2)	0.784(1)	5.2(9)

position of the pairs is different from that in RB·I_9 due to the difference in the molecular symmetry. The deformation of the RB molecule may be partly due to the π-radical formation. However, as discussed below, it is highly likely that the

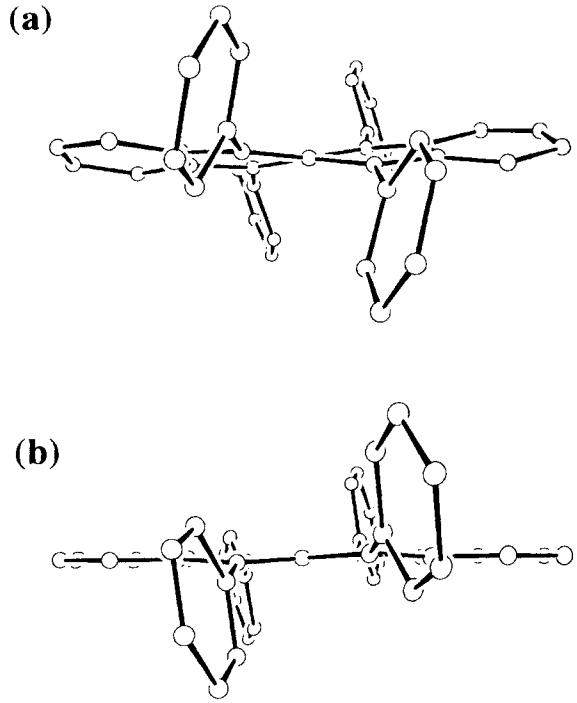

Fig. 2. The RB molecules projected along the central C–C bond; RB in RB·I_9 (a) and RB in the single component crystal (b).[9]

deformation occurs simply due to the close-packing of the components.

Figure 3 shows the crystal structure of RB·I_9. There are five iodine atoms which are crystallographically independent. I(1) locates at the inversion center (occupancy = 0.5). First, let's pay attention to the interatomic distances less than 3.0 Å. In this way, we can find two I_2 units, I(3)–I(4) (interatomic distance: 2.707(3) Å) and I(5)–I(5) (2.737(4) Å), and one I_3 unit, I(2)–I(1)–I(2) (2.920(2) Å). Since no neutral I_3 species is known, the latter unit must carry the negative charge. Secondly, we may consider the inter-unit distances less than 3.5 Å, which is recognized as the I–I chemical bond length.[10] As shown in Fig. 4, all of the I_2 and I_3 units are interconnected. The I(5)–I(5) unit bridges the I_3 units (interatomic distance: 3.460(3) Å), forming a crank-shaped one-dimensional chain along the *c*-axis. The I(3)–I(4) unit coordinates to I(2) which corresponds to the both ends of the I_3 unit (interatomic distance: 3.281(3) Å). Consequently, the branched $(I_9^-)_\infty$ chain formation occurs. The center of the I_3 unit coincides with the inversion center, and the two-fold axis passes through the middle of the bridging I(5)–I(5) unit. This polyiodide form is completely different from those of I_9^- reported before.[11–13] In general, the bond angles in polyiodides such as I_3^-, I_5^-, I_7^-, I_9^-, etc. have been found to be close to either 180° or 90°. The bond angles found in the branched $(I_9^-)_\infty$ chain are also in good agreement with this tendency, as shown in Table 3. The shortest inter-chain contact is 4.082(5) Å (I(3)···I(3)) which may be the boundary of the van der Waals contact.

In the overall crystal structure, the RB molecules and the

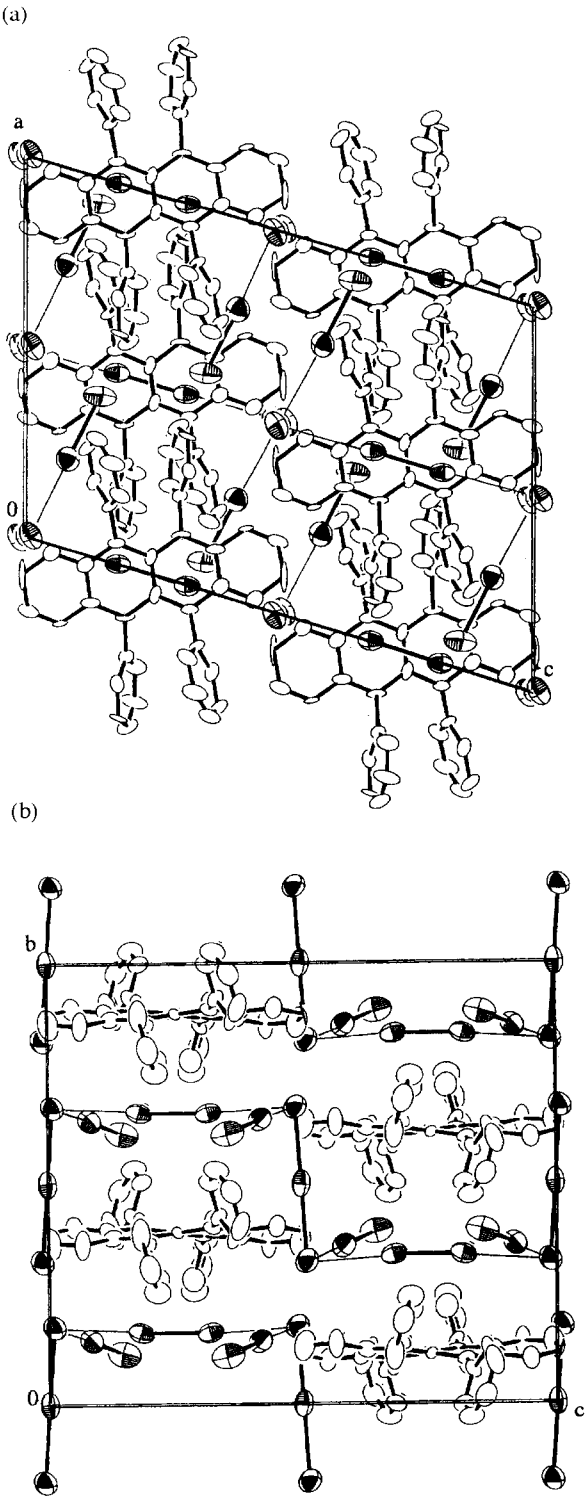

Fig. 3. The crystal structure of RB·I_9; view along the *b*-axis (a) and along the *a*-axis (b).

branched $(I_9^-)_\infty$ chains are arranged in a complicated way. As can be seen from Fig. 3, there are no intermolecular RB π–π contacts. Instead, the naphthacene plane is sandwiched by the branched $(I_9^-)_\infty$ chains. The linear I(2)–I(5)–I(5)–I(2) portion lies on the one side of the naphthacene plane, and two I(3)–I(4) portions, each of which belongs to a different

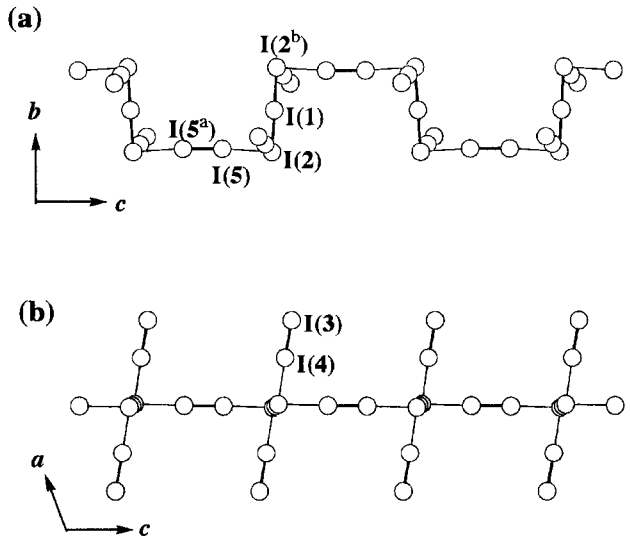

Fig. 4. Structure of the one-dimensional $(I_9^-)_\infty$ chain; view perpendicular to the *bc*-plane (a) and view along the *b*-axis (b).

Table 3. Bond Distances and Angles in the $(I_9^-)_\infty$ Chain

Bond lengths (Å)			
Atom–Atom	Length	Atom–Atom	Length
I(1)–I(2)	2.920(2)	I(3)–I(4)	2.707(3)
I(5)–I(5)[a)]	2.737(4)	I(2)–I(4)	3.281(3)
I(2)–I(5)	3.460(3)		
Bond angles (°)			
Atom–Atom–Atom	Angle	Atom –Atom–Atom	Angle
I(2)–I(1)–I(2)[b)]	180.0	I(1)–I(2)–I(4)	83.10(6)
I(1)–I(2)–I(5)	89.70(7)	I(4)–I(2)–I(5)	82.54(7)
I(2)–I(4)–I(3)	177.6(1)	I(2)–I(5)–I(5)[a)]	176.23(5)

a) Symmetry operation by the two-fold axis. b) Symmetry operation by the inversion center.

chain, lie on the other side of the plane. There are some short intermolecular contacts, such as I(3)···C(3) (3.78(2) Å) and I(2)···C(5) (3.83(3) Å). Consequently, each RB molecule is completely surrounded by the iodine chains. The RB molecular conformation seems to be rather convenient for such close packing, and the shield by the iodine chains makes it possible to isolate the stable RB radical crystals.

The significant figures of the C–C bond lengths are not enough to confirm the cation radical state of RB from the bond length change. The radical cation state has been identified by the optical and magnetic properties, as discussed below.

Infrared and Visible-Near-Infrared Spectra. When a π-conjugated molecule becomes a π-radical by oxidation or reduction, the infrared spectra generally show a dramatic change in the peak intensities and positions. This is due to the fact that the HOMO or LUMO is extended over the whole molecule and every bond order varies by the oxidation or reduction. The coefficients of the HOMO of RB has been found not to be extended over the whole molecule from the INDO calculation based on the molecular geometry obtained from the X-ray structure analysis; the HOMO is restricted only within the naphthacene ring and four phenyl rings have no coefficients. Figure 5 shows the infrared spectra of RB and RB·I_9. The latter spectrum should not contain any contribution of $(I_9^-)_\infty$, since any vibrational mode frequencies must be lower than the lowest frequency in the infrared region. In the region between 1200 and 1700 cm^{-1}, one can see the dramatic change in the spectral features. This is attributable to the RB cation radical formation, and some unchanged peaks may be the vibrational modes of the phenyl groups.

The Kubelka–Munk function, which corresponds to the absorption, obtained from the diffuse reflectance spectrum of the RB·I_9 powder is shown in Fig. 6(a). The crystal looks practically black, and indeed the absorption occurs through the whole range of the visible region. The spectrum of RB shown in Fig. 6(b) shows similar absorption bands centered at ca. 20000 cm^{-1}. Though the life-time is not long, the absorption spectrum of the RB cation radical could be recorded in the nitromethane solution by the treatment with excess aluminum chloride,[5] as shown in Fig. 6(c). Some of the bands of RB·I_9 in the near-IR region correspond well to the absorption due to the RB cation radical. Interestingly, the RB cation radical absorption bands disappeared when RB·I_9 is dissolved in benzene. The radical species is thus stable only in the RB·I_9 crystal. Though the spectrum must contain the absorption bands due to the $(I_9^-)_\infty$ species,[14] the positions cannot be determined solely from the diffuse reflectance spectrum.

Magnetic Properties of RB·I_9. As suggested from the X-ray structure analysis and IR and VIS-NIR spectra, RB in RB·I_9 becomes a π-cation radical. This is clearly demonstrated by the EPR spectra; the sharp signal with the peak-to-peak line width of 11.5 G and g = 2.006, both of which values are typical for a π-radical, was observed for the randomly oriented polycrystalline sample at room temperature. Figure 7 shows the temperature dependence of the paramagnetic susceptibility (χ_{para}) of RB·I_9 after correcting for the diamagnetic core contributions (observed value for RB and the Pascal's constants for I_9^-). Since the crystal is not stable due to loss of iodine, there might be some ambiguity in the χ_{para} values. Nevertheless, the proportion of the paramagnetic component is sufficient to conclude that

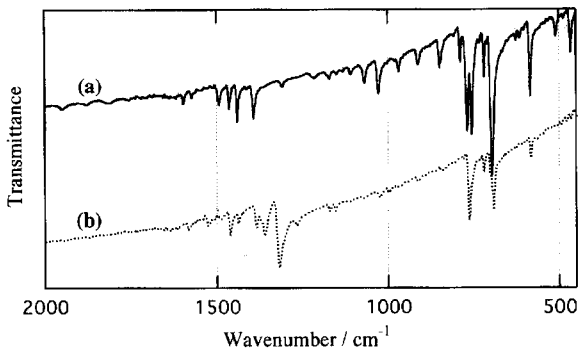

Fig. 5. Infrared spectra of RB (a) and RB·I_9 (b).

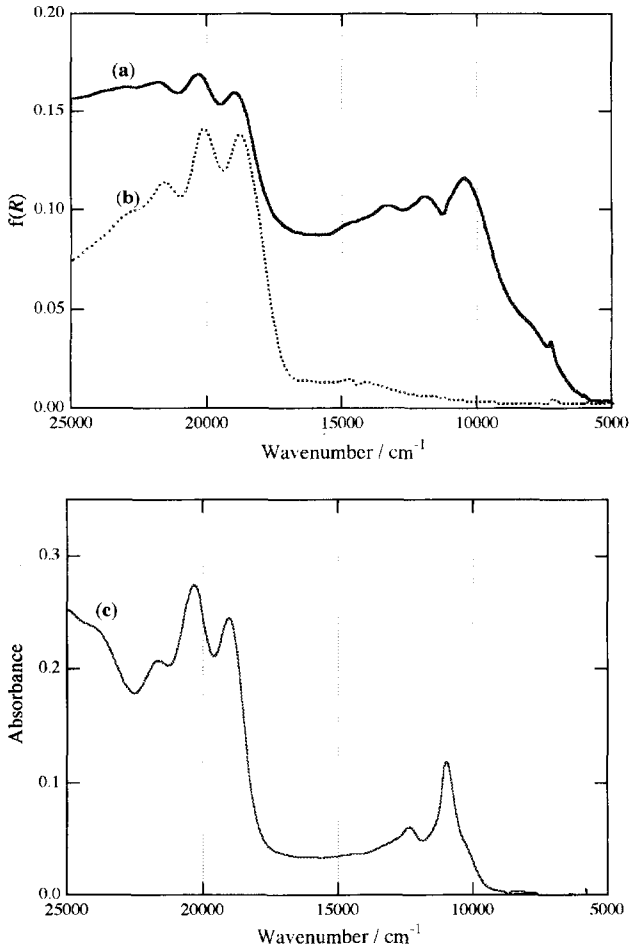

Fig. 6. VIS-NIR diffuse reflectance spectra plotted by the Kubelka–Munk function, $f(R)$, of RB·I_9 (a) and RB (b), and the absorption spectrum of the nitromethane solution of the RB cation radical produced by the treatment with aluminum chloride (c).

RB is in the cation radical state. It is rather interesting that χ_{para} shows the existence of antiferromagnetic interactions, though there are no direct contacts between the RB radicals. The solid line in Fig. 7 is the trial fitting using the Curie–Weiss law, $\chi_{para} = C/(T-\theta)$, with $\theta = -26$ K and $C = 0.279$ emu mol^{-1} K. At the present stage, the details of the magnetic exchange interactions are unknown. However, it is certain that there are some superexchange interactions through the iodine fragments overlapped with the RB π-orbitals.

In conclusion, we have succeeded in isolating the RB cation radical in the crystalline form by the complex formation with iodine. In the crystal, a unique branched crank-shaped one-dimensional $(I_9^-)_\infty$ polyiodide chain is formed. The RB radicals are completely shielded from each other by the polyiodide, and the cation radical state is stabilized. The IR, VIS-NIR, EPR specroscopies have confirmed this cation radical state, and the magnetic susceptibility measurement has indicated the existence of superexchange interactions through the polyiodide.

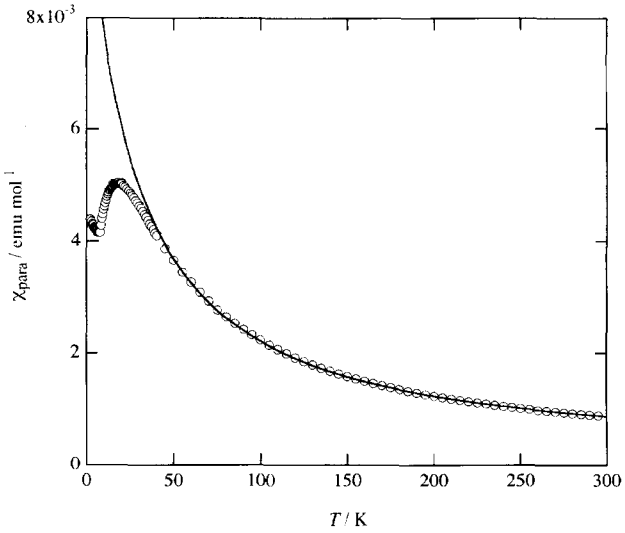

Fig. 7. Temperature dependence of the paramagnetic susceptibility (χ_{para}) of RB·I_9. The solid line is the trial fit using the Curie–Weiss law.

This work was partly supported by a Grant-in-Aid for Scientific Research No. 09874137 from the Ministry of Education, Science, Sports and Culture.

References

1 N. Sato, K. Seki, and H. Inokuchi, *J. Chem. Soc., Faraday Trans. 2*, **77**, 1621 (1981).

2 O. Neilands, K. Balodis, J. Kacens, J. Kreicberga, R. Medne, L. Paulins, G. Pukitis, V. Khodorkovsky, and A. Edzina, *Izv. Akad. Nauk Latv. SSR, Ser. Khim.*, **64** (1986).

3 N. Sato and H. Inokuchi, *Chem. Phys.*, **60**, 327 (1981).

4 A. Berlinsky, J. F. Carolan, and L. Weiler, *Can. J. Chem.*, **52**, 3373 (1974).

5 R. Biehl, K. -P. Dinse, K. Möbius, M. Plato, H. Kurreck, and U. Mennenga, *Tetrahedron*, **29**, 363 (1973).

6 "SIR92," A. Altomare, M. C. Burla, M. Camalli, M. Cascarano, C. Giacovazzo, A. Guagliardi, and G. Polidori, *J. Appl. Crystallogr.*, **27**, 435 (1994).

7 "teXsan: Crystal Structure Analysis Package," Molecular Structure Corporation (1985 & 1992).

8 The lists of the bond lengths and angles, structure factors and anisotropic thermal parameters for non-hydrogen atoms are deposited as Document No. 73003 at the Office of the Editor of Bull. Chem. Soc. Jpn.

9 I. Bulgarovskaya, V. Vozzhennikov, S. Aleksandrov, and V. Belsky, *Latv. PSR Zinat. Akad. Vestis, Khim. Ser.*, **1983**, 53.

10 F. A. Cotton and F. Wilkinson, "Advanced Inorganic Chemistry," 5th ed, John Wiley & Sons, New York (1988).

11 W. J. James, R. J. Hach, D. French, and R. E. Rundle, *Acta Crystallogr.*, **8**, 814 (1955).

12 A. J. Blake, R. O. Gould, W. Li, V. Lippolis, S. Parsons, C. Radek, and M. Schröder, *Angew. Chem., Int. Ed. Engl.*, **37**, 293 (1998).

13 K.-F. Tebbe and R. Loukili, *Z. Anorg. Allg. Chem.*, **624**, 1175 (1998).

14 M. Mizuno, J. Tanaka, and I. Harada, *J. Phys. Chem.*, **85**, 1789 (1981).